Paper accepted for presentation at 2009 IEEE Bucharest Power Tech Conference, June 28th - July 2nd, Bucharest, Romania

Evaluation of the Steady State Performance of a DC Link Built on VSC Converter Stations Using PSCAD/EMTDC©

E. Mortera-Vázquez, *student member, IEEE*, E. L. Moreno-Goytia, *member, IEEE*, L.E. Ugalde-Caballero, *member, IEEE*

***Abstract*--This paper presents a steady state performance analysis carried out to evaluate the operation and behavior of a two VSC-based level–full scale frequency converter working as a HVDC link. The digital model has been implemented and evaluated using PSCAD/EMTDC©. The emphasis of this work has been put on evaluating the transferred active and reactive power from the rectifying station to the inverting station as well as the influence of the modulation index on the total harmonic distortion (THD).**

***Index terms*--Harmonic Spectra, HVDC Stations, Pulse Width Modulation, Voltage Source Converter.**

I. INTRODUCTION

In recent years power electronic-based converters and structures has emerged with a singular strength into electrical networks applications due to a variety of causes. A primer cause relies on the necessity to efficiently utilize actual and future electrical networks. On these grounds many power electronics devices have emerged to improve the transitory, dynamic and steady state performance transmission and distribution electrical networks. An additional factor for the bulk incorporation of power electronics is pushed by the rising number of renewable generation units allocated in distribution networks, such as wind farms, medium scale photovoltaic block and even full cells generation.

In general, high-voltage direct current (HVDC) converters are a well-established technology. It is worth to note that HVDC converters are typically based on current source converter (CSC) which has some difficulties in regulating reactive power. On the other hand, converter based on a VSC can manipulate the reactive and active power independently. If the VSC based frequency converter is well designed is possible to gain some transient stability margin in a close conventional generator and to give support to ride through faults.

The author gratefully acknowledge the generous finacial support of DGEST and the Nactional Council for Science and Tehcnlogy (CONACyT) in México. Also, the excellent technical assistance of Dr. F. Rivas-Davalos and Ms. L. Marquez.

E. Mortera-Vazquez, is a student at the Instituto Tecnologico de Morelia (lalonicol204@hotmail.com)

E. L. Moreno-Goytia and L. E. Ugalde-Caballero are full-time researchers at the Instituto Tecnológicode Morelia (México) (elmg@ieee.org), (leugalde@yahoo.com.mx)

978-1-4244-2235-7/09/$25.00 ©2009 IEEE

In this work a two-level full voltage source inverter (VSC) are implemented based on power electronic switches, namely insulated gate bipolar transistor (IGBT) and a sinusoidal PWM.

II. MODULATION STRATEGY

In a conventional two-level CSC, there is only one turn-on, turn-off per switch per cycle. In such case, the ac inverter output voltage can be controlled by either manipulating the DC voltage amplitude or width of the voltage pulses [1]. An interesting approach is to have multiple pulses per each half-cycle, and then vary the pulses width to vary the amplitude of the converter ac output voltage.

Reference [2] shows a general classification of PWM's alternatives for determining the converter turn-on and turn-off proposed for fixed-frequency modulations systems.

The alternative chosen for this work is the sine-triangle modulation which is in the more common of naturally sampled PWM technique. The equation (1) helps to generate the sinusoidal signal reference needed for the DC-AC conversion [2].

$$V_{az} = M_a \cos(\omega_0 t + \theta_0) \tag{1}$$

Where:

M_a = amplitude modulation index with range $0 < M_a < 1$.

ω_0 = output frequency of the ac inverter output voltage.

θ_0 = input phase angle which determines the ac inverter phase angle of the ac output voltage.

Equation (1) is just a signal reference for phase A, for phase B and C the phase angle should be $-2\pi/3$ and $2\pi/3$, respectively.

1)-The amplitude modulation index M_a

The M_a parameter determines the magnitude of the ac output voltage, as a first approach that is a means of controlling reactive power. Equation (2) shows this concept.

$$M_a = \frac{V_{refernce}}{V_{carrier}} \quad (2)$$

Where:

$V_{refernce}$ = amplitude of the ac reference voltage (V_{az}).

$V_{carrier}$ = amplitude of the carrier triangular.

2)- The frequency modulation index M_f

The frequency modulation index must be selected to balance the switching losses against the harmonic content in the ac output voltage. A large M_f value means: 1) higher switching losses; 2) reduced low-order harmonics, and 3) high-order harmonics are shifted to the vicinity of M_f, and as consequence, they are easier to filter out. M_f is defined by equation (3):

$$M_f = \frac{f_{carrier}}{f_{refernce}} \quad (3)$$

Where:

$f_{carrier}$ = frequency of the triangular carrier.

$f_{reference}$ = frequency of the ac reference voltage (V_{az}) and it is the correspondent value in hertz of ω_0.

3)- Input phase angle θ_0

The phase angle determines if the converter is operating as rectifier or as inverter. In addition, manipulating this parameter it is also achievable operate the converter in any of the four quadrants.

III. Active and Reactive Power Flow

From the point of view of the electrical network, a VSC structure behaves as a very fast controllable synchronous machine to which its amplitude, phase angle and frequency of its ac output voltage can be independently controlled. Equation (4) describes the instantaneous output phase voltage [3]:

$$V_{2i} = \frac{1}{2} V_{dc} M_a \sin(\omega_0 t + \varphi_0) + harmonic\ terms \quad (4)$$

Where:

V_{dc} = DC voltage at the DC link.

φ_0 = phase shift angle of the ac output voltage dependable of θ_0 from the reference voltage.

As equation (4) indicates, the voltage generated contains a fundamental voltage and harmonics components. Considering the condition that the output voltage pulses are symmetrical around the zero-crossing point of the current signal, then the even harmonics can be eliminated if M_f value is chosen as an odd integer multiple of the fundamental frequency. Moreover, if M_f is selected as multiple of three, a factor representing the number of phases, then all harmonics multiples of three should be equal in magnitude and phase, and as a consequence the phase-to-phase voltage harmonics are eliminated becoming zero sequence harmonics.

V_{2i} may represent an A, B or C phase voltage where the phase difference is determined by φ_0. As M_a and φ_0 values can be independently adjusted then the voltage across the reactor (ΔV_{Xi}) can be thoroughly varied to control active and reactive power flow through the converter. The reactor size, calculated once ΔV_{Xi} is obtained, can help determining the maximum reactive and active power to be injected or absorbed, in steady or dynamic state, by the converter. Fig. 1 illustrates a VSC based converter in PSCAD including the main parameters governing reactive and active power flow.

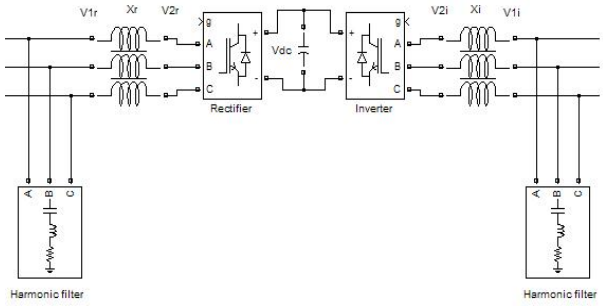

Fig. 1. Full scale power converter based on VSC showing its main components.

Equations (5) and (6) determine, respectively, the active power and reactive power [3]. V_{2i} and V_{1i} correspond to fundamental phase to phase voltages.

$$P = \frac{V_{2i} V_{1i} \sin\varphi_0}{X_i} \quad (5)$$

$$Q = \frac{V_{2i}(V_{2i} - V_{1i}\cos\varphi_0)}{X_i} \quad (6)$$

As can be notice, if X_i is fixed the active power and the reactive power can be respectively controlled by φ_0 and V_{2i}, and the magnitude of V_{2i} depends on V_{dc} and M_a.

IV. Implementation of the Modulation Strategy

Fig. 2 shows the implementation in PSCAD/EMTDC™ of the modulation strategy for the VSC Stations DC-Link.

A relevant to mention building block is the interpolated firing pulses block. This component provides the firing pulses and the interpolated time tag in the form of a two-

element array. The first array element is the IGBTS control signal, that is, the firing pulses.

The second array element is the exact runtime, in seconds, at which IGBT transition occurs, in relation to a fixed step grid simulation [4, 5]. The manipulation of such parameter allows using larger simulation step times with no loss of accuracy. Any other IGBT firing alternative requires small step times which compromise accuracy. However, whichever IGBT firing technique is used, losses should be kept into realistic margins.

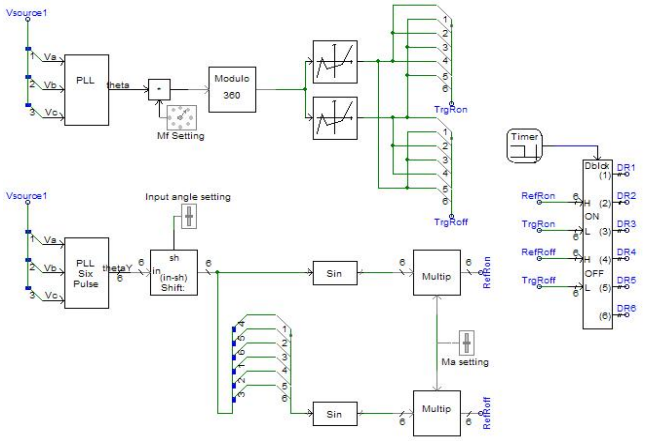

Fig. 2. Implementation of the modulation strategy

The phase locked-loop (PLL) shown in Fig. 2 is a playing part with the interpolated firing pulses block for implementing the sine-triangle modulation. Fig. 3 illustrates the resulted sinusoidal-PWM for a single phase.

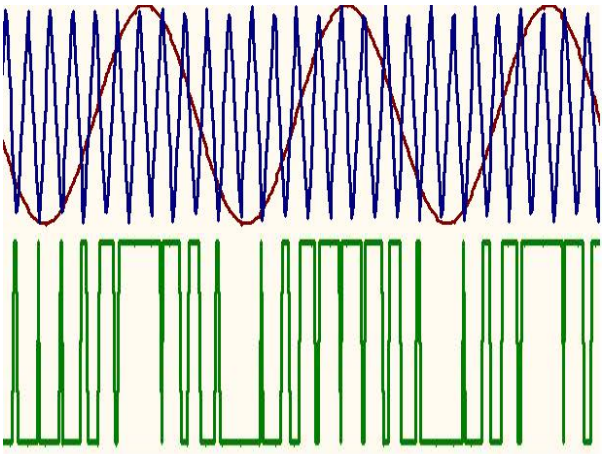

Fig. 3. SPWM frame.

V. Stand Alone Performance of the Voltage Source Converter

Fig. 4 illustrates a VSC-Based Converter Station. The converter is operating as inverter and no load is connected at the AC side. In this case the DC voltage is supplied by two ideal 5 kV voltage sources.

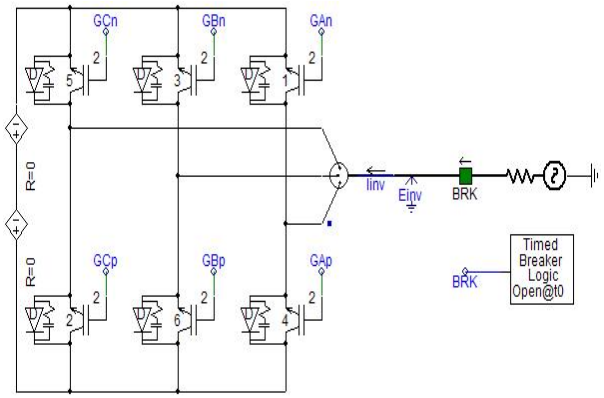

Fig. 4. A VSC Structure

A test case has been carried out using M_a=1, M_f=9, $\theta_0 = 0$, and $\omega_0 = 377$ (rad/s).

Fig. 5 shows the phase to neutral voltage A and the reconstructed fundamental frequency component, obtained with the FFT. For the other phase to neutral voltages the waveform are similar. The original wave form seems to be a three level by each halve cycle, in fact it does, however it is due to the voltage is measured against a fictitious reference point and not against the common point of the two ideal sources. Because the reference signal has a phase angle of 0 degrees, this is $\theta_0 = 0$. The ac output voltage for phase A is 180° out of phase the signal reference phase angle.

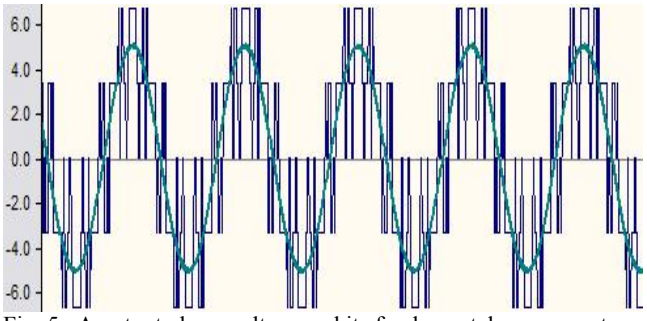

Fig. 5. A output phase voltage and its fundamental component.

Fig. 6 pictures the waveform of the phase to phase voltage AB along with the fundamental frequency component.

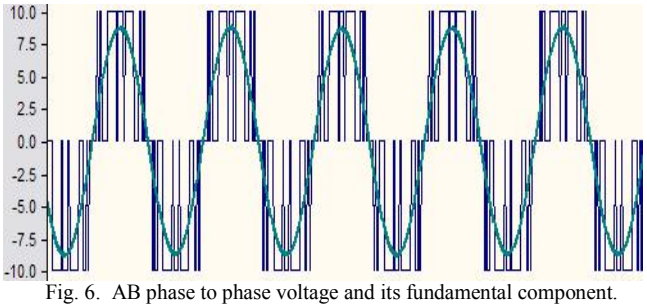

Fig. 6. AB phase to phase voltage and its fundamental component.

Fig. 7 shows the harmonic spectra of the non-filtered phase to neutral voltage A. The THD for the non-filtered signal is 54%. Similar results apply to the others phases and for phase to phase voltages.

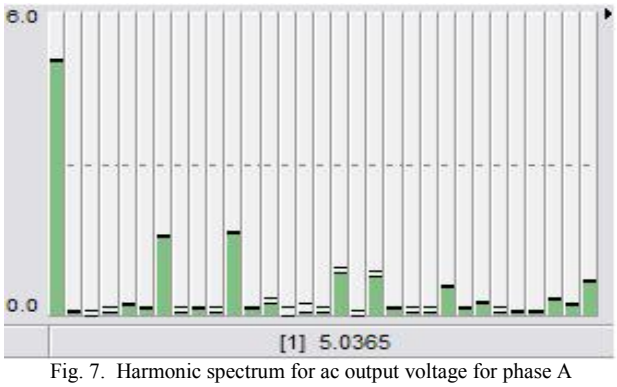

Fig. 7. Harmonic spectrum for ac output voltage for phase A

Table I shows the phase angle changes in phase to neutral voltages and phase-to-phase voltage relative to changes in θ_0. This table also illustrates the four quadrant operation of the VSC. Considering a fixed voltage magnitude of any phase, it can be notice in Table 1 that the first quadrant starts at $\theta_0 = 0$ and end in $\theta_0 = 90$ injecting active power to the ac system. The second quadrant starts at $\theta_0 = 90$ ending in $\theta_0 = 180$ injecting active power to the ac system. The third quadrant starts at $\theta_0 = 180$ finishing in $\theta_0 = 270$ but consuming active power from the ac system. Finally the fourth quadrant starts $\theta_0 = 270$ and ends in $\theta_0 = 360$ also consuming active power to the ac system

TABLE I. RELATIONSHIP BETWEEN INPUT PHASE ANGLE AND PHASE VOLTAGE OUTPUTS

Input phase angle (θ_0)	Phase angle (φ_0) for phase voltage	Phase angle for phase to phase voltage
0.00	180.00	30.00
30.00	150.00	0.00
60.00	120.00	330.00
90.00	90.00	300.00
120.00	60.00	270.00
150.00	30.00	240.00
180.00	0.00	210.00
210.00	330.00	180.00
240.00	300.00	150.00
270.00	270.00	120.00
300.00	240.00	90.00
330.00	210.00	60.00
331.00	209.00	59.00
360.00	180.00	30.00

Table 2 shows the relationship between the value of M_a and the effects on the THD and the fundamental RMS value of both the phase, and the phase to phase voltage.

TABLE II. THD AND RMS PHASE VOLTAGE AS A FUNCTION OF M_a

Ma	THD (%)	RMS phase voltage
1	54	3.56
0.95	57	3.41
0.9	62	3.2
0.85	66	3.02
0.8	72	2.82
0.75	77	2.68

VI. PERFORMANCE OF A FULL BACK-TO-BACK POWER STATIONS

Fig. 8 shows the AC-DC-AC stud-case testing network implemented in PSCAD. The test system is made of two infinite bus systems of 0.48 kV. Each AC system has a step-up transformer of 0.48/10.0 (kV), having a leakage of 0.01 (per unit using 2 MVA as base) and a grounded-wye/delta connection. The two AC systems are interconnected along using a VSC-based DC link.

In order to minimize voltage and current distortion in the AC-VSC interface area, a low pass filter is installed in each side of the VSC-based power converter. Each filter has a 50 μf capacitor and a 0.1 Hy inductor per phase connected in between the transformer and the power converter connected both in a wye-grounded connection.

The dc link interface is made of two of 375 μf capacitors each one, having a neutral point between them.

As have been aforementioned, a VSC has four operative quadrants where the lagged 30° degrees caused by the wye-delta connection should be taking into account, which means actually any of the four quadrants begins 30° degrees out of phase. Under these conditions it should be notice that for rectifier operation the most convenient phase angle (θ_0) for the input shall be 120° degrees and values in the neighborhood. On the other hand, for a suitable inverter operation a phase angle θ_0 around 300° degrees is a right choice. As can be notice, the inverter and rectifier VSC operation is 180° out of phase.

As an evaluation of the VSC-Based link performance, a test case has been carried out using M_a=1 and M_f=9. For the VSC operation as rectifier, a $\theta_0 = 300°$ is used in one VSC-based station and for inverter operation of the second VSC-based station a $\theta_0 = 120°$ is used

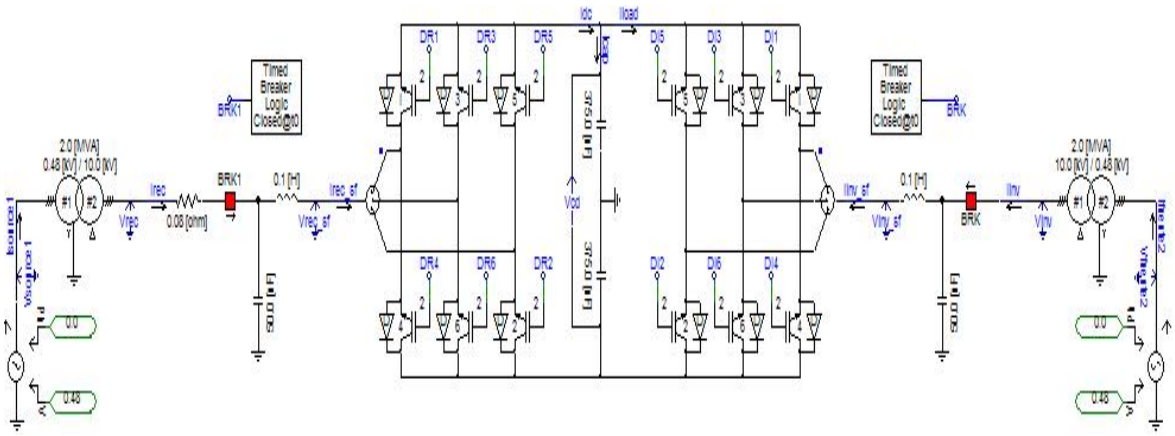

Fig. 8. Full scale power converter based VSC showing all the electrical components

Fig. 9 shows the DC voltage at the DC link interface. This voltage tends to stabilize in the vicinity of 10.6 kV.

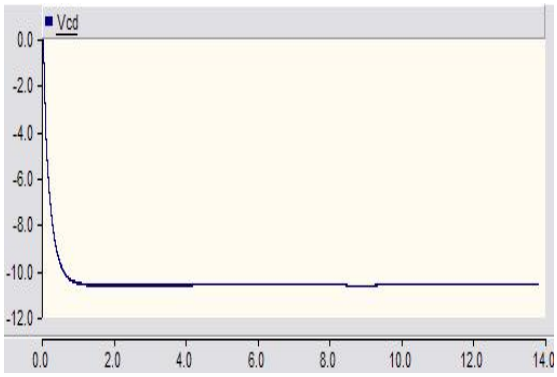

Fig. 9. Voltage at the dc link

Fig. 10 illustrates the active power flowing from the side rectifier station side to the DC link and the active power flow flowing through the inverter from such DC link. The active power injected to the DC is 1.73 MW whereas the active power absorbed by the inverter is 1.70 MW.

The closeness between the injected and ejected active power into the DC link is an indicative of a proper system operation. However, the relative small difference shown in Fig. 10 is an evidence of IGBT commutation losses in both rectifier and inverter stations. For this case such losses are approximately 1.73% of total active power being evenly distributed between conversion stations.

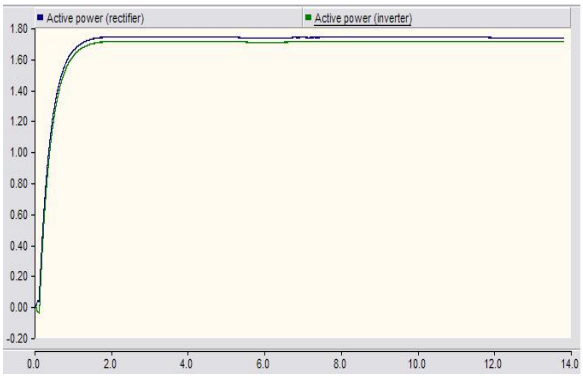

Fig. 10. Active power flow at side rectifier and at side inverter

Fig. 11 and Fig. 12, show the AB phase to phase voltage at rectifier side and at side inverter, respectively. As can be notice, both voltage waveform are distorted but they are reconstructed by filtering.

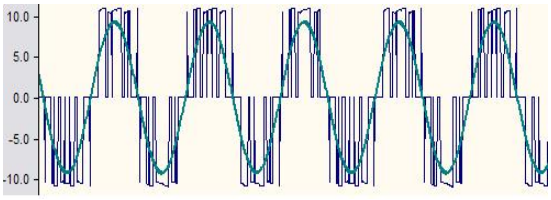

Fig. 11. Phase to phase voltage AB and its fundamental component for side rectifier.

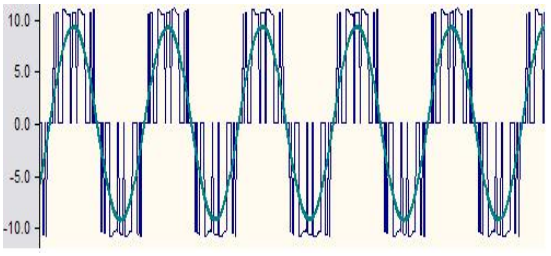

Fig. 12. Phase to phase voltage AB and its fundamental component for side. Inverter.

Fig. 13 and Fig. 14, show the harmonic components for AB phase to phase voltage at side rectifier and at side inverter, which THD is 38 % and 44 % respectively.

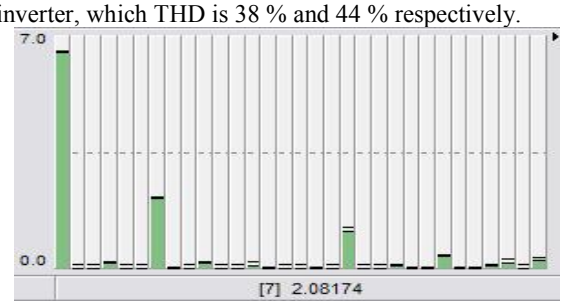

Fig. 13. Harmonic spectra for AB phase to phase voltage component for side rectifier

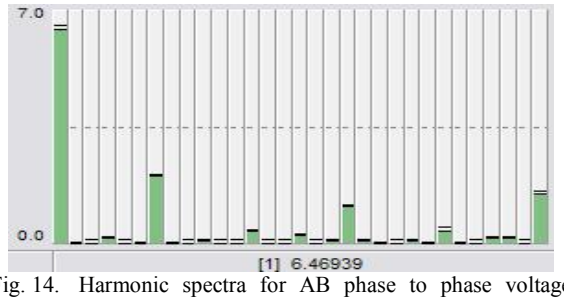

Fig. 14. Harmonic spectra for AB phase to phase voltage component for side inverter.

In Fig. 15 is presented how to measured active and reactive power in presence of distorted waveforms, here is implemented the traditional formula but is possible to implement (5) and (6) knowing the fundamental phase to phase voltages at each side of the inductor plus the angular difference between one pair of the fundamental phase voltages at each side of the inductor too. The voltages and currents per phase measured are passed through a FFT that calculates the fundamental component and their shift phase angle in order to calculate the power factor (PF). The FFT block calculates the positive sequence voltage in order to account any unbalance between phases.

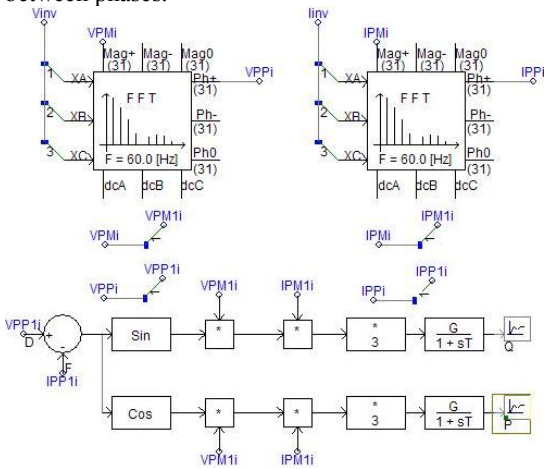

Fig. 15. Calculation of active and reactive powers considering distorted waveforms.

VII. Conclusions

This work has been served to identified the four quadrants operation of a voltage source converter working as a voltage source inverter, this led to choose the best shift phase angle of the input phase angle (θ_0) to operate the rectifier and the inverter of a full scale power converter based on a voltage source converter. More over, it has been investigated how changed the total harmonic distortion as a function of the amplitude modulation index plus how to measured active and reactive power in presence of distorted waveforms.

VIII. References

[1] N. G. Hingorani, "Understanding FACTS, concepts and technology of flexible ac transmission systems", IEEE Press, 2000, pp. 91-95.

[2] D. G. Holmes, "Pulse width modulation for power converters, principles and practice", IEEE Press, 2003, pp. 105-113.

[3] Cuiquing Du, "The control of VSC-HVDC and its use for large inductrial power systems", Thesis of licentiate of engineering, department of electric power engineering, Chalmers University of Technology, Göteborg, Sweden, 2003, pp. 18-20.

[4] G.D. Irwin, D.A. Woodford & A. Gole, "Precision simulation of PWM controllers", Manitoba HVDC Research Centre Inc, available: http://www.hvdc.ca/pdf_misc/IPST1231.pdf

[5] Manitoba HVDC research center, Inc., "PSCAD on-line help system", PSCAD/EMTDC™ Version 4.2, November 16, 2005.

IX. Biographies

Edgar L. Moreno-Goytia (M´95) was born in northern México on June 12, 1966. He graduated as an Electronics and Communications Engineer from the National Politechnique Institute (México) on 1993. He also holds a PhD on Electrical Engineering, graduated from Glasgow University (UK) on 2003.
His academic experiences include DC links, multilvel-VSC and distributed generation.

Eduardo Mortera-Vazquez was born in Veracruz, Mexico. He graduated as an Electrical Engineer from the Instituto Tecnologico de Orizaba. He is currently completing his Master in Science Thesis on Stability of Distribution Networks with disperse generation at the Instituto Tecnologico de Morelia (Mexico).

Luis E. Ugalde-Caballero was born in Morelia, Mexico. He has a bachelor and master in science degree from the Instituto Tecnologico de Morelia. Presently, he is pursuing a PhD degree on HVDC converters from the Michoacana University (México).